Very Low Frequency, Low Power Oscillators

S F Al-sarawi
P H Cole
D Abbott
Department of Electrical and Electronic Engineering, University of Adelaide, SA

A new technique to extend the integration voltage of the relaxation oscillator is described. The technique is based on using N integrators rather than a single integrator in the oscillator. This results in the extension of the integration voltage of the integrators from rail-to-rail instead of restricting it to the Schmitt trigger hysteresis width. Experimental results of a new variant of the Schmitt oscillator, that operates at 52Hz using 5V supply voltage, are presented.

1 Introduction

Oscillators are basic building blocks in a wide range of applications, whether these applications are analog or digital. They can be classified in a number of ways. For example, they can be classified according to high, medium and low frequency of operation, or according to the output waveform type (square-wave sine-wave, etc.) The type of oscillator which will be discussed here is the low frequency, square wave relaxation oscillator. This oscillator consists of two switched current sources, a capacitive load and a dual voltage reference comparator. The combination of the switched current sources and the capacitive load forms an integrator. As the dual reference comparator in the design of the relaxation oscillator can be replaced by a Schmitt trigger circuit, some people refer to oscillators using Schmitt trigger circuits as "Schmitt-Oscillators." A simplified schematic diagram of the Schmitt-oscillator is shown in Figure 1. An extra inverter is used at the Schmitt trigger output in order to obtain the right phase at the input terminals of the switched current sources.

Schmitt-oscillators are commonly used in CMOS technology because: (i) they are very well suited for integration; (ii) they have a simple structure and (iii) the frequency of oscillation can be adjusted and tuned using an electrical signal. As most portable applications have a limited energy source, much attention has been directed to designing low power circuits and low voltage oscillators. This is especially so, in the case of oscillators, as they are basic building blocks in most analog and digital systems.

In this paper the authors present a new design technique for designing very low frequency Schmitt-oscillators. As the new technique will be employed in the design of Schmitt-oscillators, a brief analysis of the Schmitt-oscillator will be presented in Section 2. Based on the presented analysis, the new design technique and its application in the design of a new variant of the Schmitt-Oscillator is discussed in Section 3. Section 4 presents experimental measurements for the new variant of the Schmitt-Oscillator.

2 Schmitt-Oscillators

The principle of operation of the Schmitt-Oscillator, shown in Figure 1, can be described as follows. Assuming a zero charge across C_L, the voltage at the input of the Schmitt trigger circuit, V_C, is low, hence the output of the Schmitt trigger is high, forcing S_{ch} to switch "ON" and S_{disch} to switch "OFF." So, C_L starts to charge linearly using current I_{ch}. Once the V_C reaches the Schmitt trigger V_{HL}, which is the input voltage at which the output of the Schmitt trigger switches from high to low, the output of the Schmitt trigger switches very rapidly from high to low, complimenting the states of S_{ch} and S_{disch}. Now, C_L starts to discharge using I_{disch}. Once the voltage across C_L reaches the Schmitt trigger V_{LH}, which is the input voltage at which the Schmitt trigger output switches from low to high, the output of the Schmitt trigger changes its state. Then, the cycle continues with an initial voltage across C_L equal to V_{LH}. The oscillation frequency, f_o, of this oscillator can written as

$$\frac{1}{f_o} = C_L V_{HW} \left(\frac{1}{I_{ch}} + \frac{1}{I_{disch}} \right)$$

Where V_{HW} represents the hysteresis width of the Schmitt trigger circuit which is defined as $V_{HL} - V_{LH}$. To obtain a fully symmetrical square waveform from the oscillator the charging and discharging currents should be equal. *ie.* $I_{ch} = I_{disch} = I_b$. So, the above equation can be written as

$$f_o = \frac{1}{T_o} = \frac{I_b}{2C_L V_{HW}} \tag{1}$$

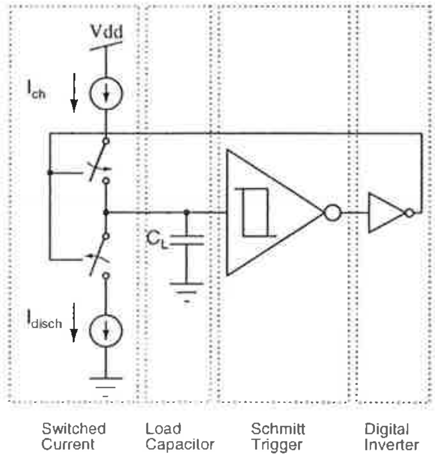

Figure 1: A schematic diagram of the conventional integrator oscillator.

The highest frequency that the Schmitt-oscillator can deliver is obtained by maximising the ratio of I_b to $C_L V_{HW}$. It has been reported that an oscillation frequency in the range of 1 GHz is achieved [1, 2] using this type of oscillator. Even though the challenge in most applications is in the design of high frequency oscillators, there is another challenge, namely the design of very low frequency oscillators. The low frequency limit is bounded by the smallest controlled current that can be generated on chip and the largest practical capacitor size that can be integrated on chip. For example, if the hysteresis width of the Schmitt trigger is 5/3 Volts, the smallest control current that can be generated is 1 nA and the largest practical capacitor size is set to 10 pF, using Equation 1, the lowest obtainable oscillation frequency is 30 Hz. To obtain a lower frequency value either the current limit or capacitor size has to be stretched. An alternative solution is to use a digital frequency divider circuit. However, the use of a digital divider is costly in terms of silicon area as the average number of transistors in such circuits is around 20-24 transistors [3]. The solution proposed in this paper is to extend the integration voltage of the integrator to be from rail-to-rail. This technique is discussed in details in the following section.

3 Extended Mode Schmitt-Oscillator

The new technique will be described through the design of a new variant of the Schmitt-Oscillator. The new oscillator is called "Extend Mode Schmitt Oscillator" and will be referred to as EMSO. The EMSO has an oscillation period larger than the conventional Schmitt-oscillator, when using the same bias current and an equivalent capacitor size. This is achieved through using N integrators instead of one to extend the integration voltage from rail-to-rail rather than restricting it to the Schmitt trigger hysteresis width of the Schmitt trigger circuit, as will be shown in the following analysis.

The oscillation frequency of the new oscillator, shown in Figure 2, as a result of using N integrators can be found using the resultant integration times, T_{o_e}, during the charge, T_{ch}, and discharge, T_{disch}, phases. Firstly, during the charging period, T_{ch}, C_1 to C_N will be charging to V_{dd} using a constant current source, I_{ch}. However, C_{i+1} will start charging when the voltage across C_i reaches the Schmitt trigger V_H voltage. So, the charging times T_{ch} as function of the capacitor values can be written as

$$T_{ch} = \frac{V_H}{I_b} \sum_{i=1}^{N} C_i \tag{2}$$

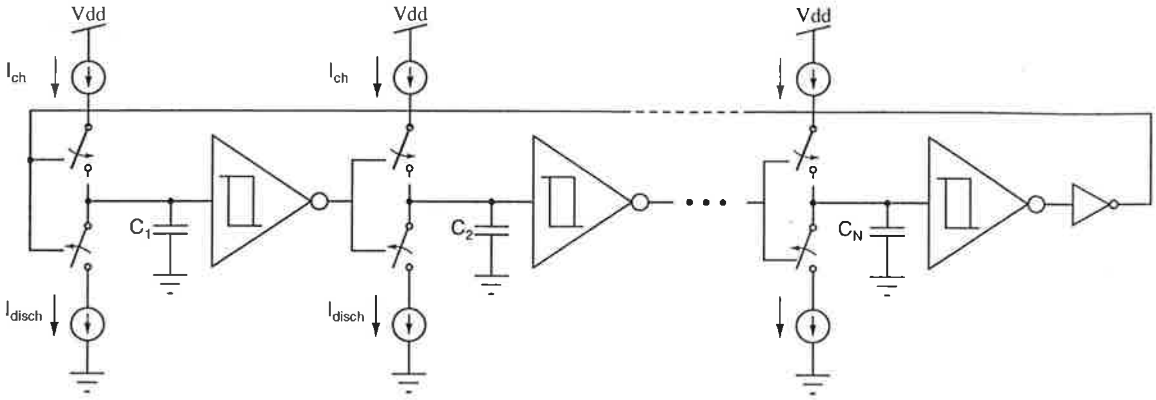

Figure 2: A schematic diagram of the extended mode integrator oscillator (EMSO).

Secondly, using the same procedures the discharge time can be written as

$$T_{disch} = \frac{V_{dd} - V_L}{I_b} \sum_{i=1}^{N} C_i \tag{3}$$

So, using Equations 2 and 3, T_{o_e} can be written as

$$T_{o_e} = \frac{2V_{HW}}{I_b} \left[\frac{V_{dd}}{2V_{HW}} + \frac{1}{2}\right] \sum_{i=1}^{N} C_i \tag{4}$$

To show the increase in the oscillation period as a result of using the extended mode technique, Equation 4 can rewritten in terms of Equation 1, with assumption that the $\sum_{i=1}^{N} C_i$ equals C_L in the common Schmitt-oscillator, as

$$T_{o_e} \quad = \quad T_{os} \left[\frac{V_{dd}}{2V_{HW}} + \frac{1}{2}\right] \tag{5}$$

Equation 5 shows that the oscillation period of the EMSO will always be larger than the oscillation period of the conventional Schmitt-oscillator. For example, if the same values of I_b and V_{HW} in the example discussed in Section 2 with C_T is set to 10 pF are used in calculating the oscillation frequency of EMSO, the resultant oscillation frequency will be 15 Hz. So the oscillation frequency is half that obtained using the conventional Schmitt-oscillator. This difference in frequency can be translated in terms of area reduction of the capacitor size needed, *ie.* only a 5 pF capacitor is needed to obtain a 30 Hz oscillation. The true saving as a result in using this technique is less than 50% due to the overhead of using another Schmitt trigger and switched current sources. So, the optimum number of integrators that are needed to still extend the integration voltage of the integrators from rail-to-rail is two. In general the saving is well above 25% and depends on the supply voltage and the hysteresis width of the Schmitt trigger circuit.

Commonly used Schmitt trigger circuits do consume a large amount of current from the power supply [4, 5, 6]. By using the very low power Schmitt trigger circuit designed by the authors in a previous publication [7], the overall power can be reduced dramatically as the maximum switching current of this Schmitt trigger circuit is less than 1 μA at 5 Volts supply.

4 Experimental Results

For reasons related to the targeted application, which is a radio frequency identification system, there is an interest in the linear triangular waveforms across the capacitors, in addition to the square output of the EMSO. However, the needed number of linear triangular waveforms is five. So, instead of using the optimal number integrators in the design of the oscillator another 3 integrators were used. The load capacitance for every integrator was chosen to be 0.8 pF, resulting in a total capacitance of 4 pF. This circuit was fabricated in the Orbit 2 μm double poly, double metal standard n-well CMOS technology through MOSIS. For the oscillator design, I_{ch} and I_{disch} were set to be equal to obtain a square wave output. The size of the fabricated oscillator is 0.048 mm^2 excluding the reference bias circuit.

A special startup mechanism was incorporated in the oscillator to guarantee the oscillator starts and to synchronise the initial charge across all the capacitors. This startup circuit is simply an nMOS transistor across every capacitor with the gates of all the nMOS transistors tied together and controlled externally. For a fully integrated oscillator, an astable multivibrator can be used to generate a high pulse for a small period of time to initialise the voltage across the capacitor. This approach was not adopted in the test oscillator as the interest is to test the functionality of the oscillator. The bias current for the oscillator was generated using the bandgap reference current-voltage presented in [8]. The bias current of 3.65 nA was measured using a Keithly 236 source-measure unit.

The measured output waveform at 3 Volts supply is shown in Figure 3. Furthermore, the measured oscillation frequency as function of the supply voltage is shown in Figure 4. As can be seen from the figure, the oscillation frequency is inversely proportional to the supply voltage. This inverse relation is due to the following factors. Firstly, it is due to the new oscillator structure, resulting in an oscillation frequency that is function of the supply voltage (as can be seen from the analytical expression for the oscillation frequency given in Equation 4.) Secondly, it is due to the increase in the hysteresis width of the Schmitt trigger circuit as function of the supply voltage. Combining these factors with the fairly constant bias due to the use of the bandgap reference voltage circuit in the generation of the bias current explains the inverse relation shown in the figure.

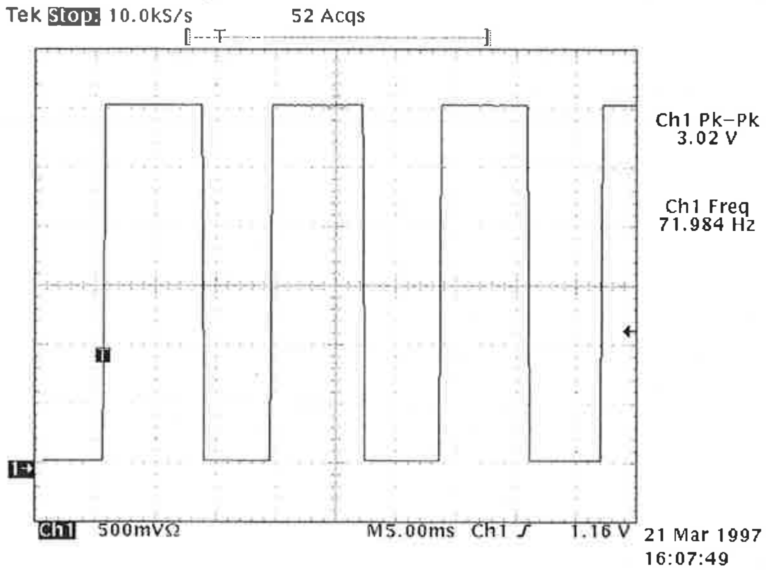

Figure 3: The measured oscillation frequency of the EMSO which uses five integrators at 3 Volts supply voltage.

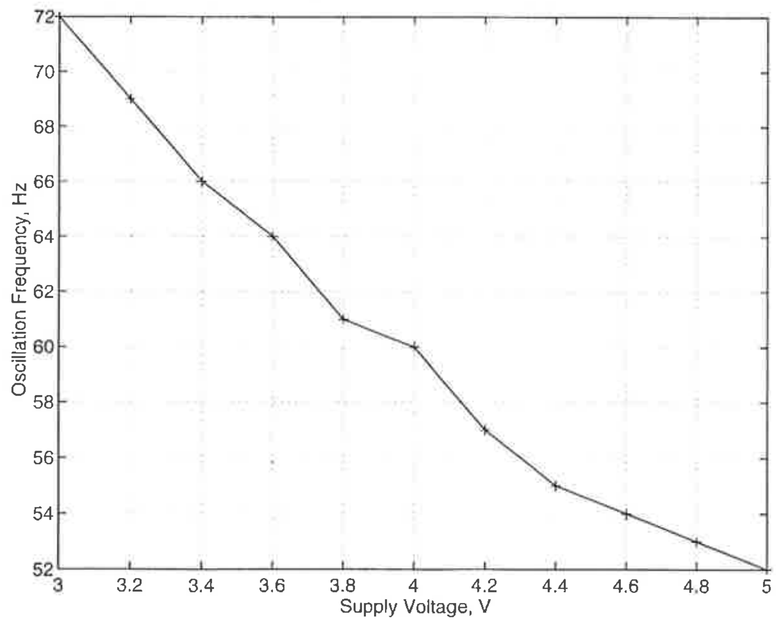

Figure 4: The measured oscillation frequency of the EMSO as function of the supply voltage.

5 Conclusion

In conclusion, a new design variant of the Schmitt-oscillator was discussed. This technique extends the integration voltage of the Schmitt-oscillator from rai-to-rail. Using this approach it is possible to design a Schmitt-oscillator that has an oscillation frequency lower than the one achieved using the conventional Schmitt-oscillator when using the same bias and capacitor size reduced by 30-50%. This factor depends on the ratio of the hysteresis width of the Schmitt trigger circuit to the supply voltage as dictated by the presented analysis. Combining the low power Schmitt trigger circuit design by the authors in a previous publication, it is possible to dramatically reduce the overall power dissipation of the oscillator as the Schmitt trigger circuit is the only "current hungry" component in the oscillator design. Experimental results are in agreement with the presented analysis and indicate that, in addition to the square wave output of the circuit, the very linear truncated triangular waveform that extends from rail-to-rail at some of the oscillator internal nodes can be useful for some applications as was demonstrated for the targeted application.

6 Acknowledgement

The authors would like to thank Integrated Silicon Design Pty. Ltd. for supporting this work and providing funds for a tiny chip fabrication.

References

[1] M. Banu, "MOS oscillators with multi-decade tuning range and gigahertz maximum speed," *IEEE Journal of Solid-State Circuits*, vol. 23, no. 6, pp. 1386- 93, 1988.

[2] B. Razavi, "A study of phase noise in CMOS oscillators," in *IEEE J. Solid-State Circuits*, vol. 31, pp. 331–43, IEEE 1995 Custom Integrated Circuits Conference, IEEE, 1996.

[3] N. Weste and K. Eshraghian, *Principles of CMOS VLSI Design*, ch. 2, pp. 115–9. VLSI systems series, Addison-Wesley, 1985.

[4] B. Dokic, "CMOS schmitt triggers," *IEE Proceedings G (Electronic Circuits and Systems)*, vol. 131, pp. 197–202, October 1984.

[5] Z. Wang, "CMOS adjustable schmitt triggers," *IEEE Trans. Inst. meas.*, vol. 40, pp. 601–605, June 1991.

[6] Z. Bundalo and B. Dokic, "Three-state CMOS schmitt triggers," *International Journal of Electronics*, vol. 66, pp. 81–92, January 1989.

[7] S. Al-Sarawi and P. Cole, "Three new schmitt trigger circuits with adjustable hysteresis," in *Proceedings of MICROELECTRONICS 1993*, (Gold Coast, Qld., Australia), pp. 239–44, Dept. of Electr. & Electron. Eng., Adelaide Univ., SA, Australia, Inst. Radio & Electron. Eng; Edgecliff, NSW, Australia, October 1993.

[8] E. Vittoz, "The design of high-performance analog circuits on digital CMOS chips," *IEEE J. Solid-State Circuits*, vol. 20, pp. 657–65, June 1985.